ON THE OPTICAL CONSTANTS OF METALS AT WAVELENGTHS SHORTER

THAN THEIR CRITICAL WAVELENGTHS*

W. R. Hunter [1963] 30 p

E. O. Hulburt Center for Space Research

U. S. Naval Research Laboratory, Washington, D. C.

1688944

To be presented at

(NASA Order R-107)

(NASA CR-53153)

******

(7140-PRR-3/63; 1570-1103-3/63)

ON THE OPTICAL CONSTANTS OF METALS AT WAVELENGTHS SHORTER

THAN THEIR CRITICAL WAVELENGTHS*

W. R. Hunter
E. O. Hulburt Center for Space Research
U. S. Naval Research Laboratory, Washington, D. C.

SUMMARY

15364 A

The optical properties of Al, In, Mg, and Si have been investigated in the extreme ultraviolet at wavelengths shorter than their critical wavelengths. It was found that Al, Mg, and Si, which have loosely bound valence electrons and tightly bound core electrons can be described, to a good approximation, by the free electron theory. For In, in this spectral range, the dominant term in the complex dielectric constant is the free electron term, however, other absorption mechanisms are not negligible so a simple two-parameter theory cannot be used.

INTRODUCTION

One of the consequences of Maxwell's theory of the propagation of

electromagnetic waves in a medium containing free charges is the existence

of a critical wavelength λ_c . Wavelengths greater than λ_c are reflected

while the shorter wavelengths penetrate into the medium. A simple explana-

tion of λ_c is that the free charges oscillate in phase with the electromagnetic

waves for $\lambda > \lambda_c$ but are π radians out of phase for $\lambda < \lambda_c$. Thus the

energy reradiated by the oscillating charges interferes constructively with

the transmitted wave and destructively with the reflected wave for $\lambda < \lambda_c$

and vice versa.

In the case of a metal, the free charges are electrons which, by virtue

of their coulomb interactions, are capable of collective oscillations.

Consequently it is to be expected that metals will have a λ_c given by;

$$\lambda_c = \frac{c}{e} \sqrt{\frac{\pi}{N}}$$

where c is the velocity of light, e is the electronic charge and N the

valence electron density.

This simple model was used by Zener (1) to explain the experimental

results of Wood (2) who showed that the alkali metals are transparent in

the ultraviolet. This theory was successful in that it gave fair approxima-

tions to the observed wavelength at which transmission set in. However, it

requires total reflection at all angles of incidence for $\lambda > \lambda_c$ which is not

the case. Kronig (3) modified Zener's theory by introducing damping of the

free electron motion, due to collisions with the lattice. This then becomes

the free electron theory of Drude (4) and, for the purpose of describing

optical phenomena, can be put into the following form:

$$\epsilon_1 = n^2 - k^2 = 1 - \frac{\omega_c^2 \tau^2}{1 + \omega^2 \tau^2} \tag{1}$$

$$\epsilon_2 = 2nk = \frac{1}{\omega_c \tau} \frac{\omega_c^2 \tau^2}{1 + \omega^2 \tau^2} \tag{2}$$

In the limit as τ approaches infinity, Eq. (1) becomes:

$$\epsilon_1 = n^2 = 1 - \frac{\omega_c^2}{\omega^2} \tag{3}$$

and Eq. (2) becomes zero, i.e., Zener's model. ϵ_1 and ϵ_2 are the real

and imaginary parts of the complex dielectric constant, respectively; n is

the index of refraction, k is the extinction coefficient, ω_c is the critical

angular frequency and τ is the relaxation time of the electrons.

A Drude type model describes fairly well the optical properties of the

alkali metals which have a loosely bound valence electron and tightly bound

core electrons (5). Hence, it is reasonable to expect that the theory would

3

be at least a good first approximation to other metals that have loosely bound valence electrons and tightly bound cores. Pines (6) discussed the classification of metals by the binding energy of the valence and core electrons and found that the metals listed in Table I have this characteristic in common with the alkali metals. Thus the inference can be made that a critical wavelength exists for these metals at which transmission should commence. In Table I is listed, for several elements, the value for λ_c and the nearest absorption edge at which k should once again become large enough to reduce or prevent transmission.

Metals that cannot be described by the free electron theory may still have a λ_c accompanied by transmission for $\lambda < \lambda_c$. This means that the free electron term in the complex dielectric constant is dominant in the region around λ_c, however, other absorption processes will not be far enough removed from the region to be negligible. Some examples are indium, tin, antimony, and bismuth. Other metals, such as gold (7), have no optical transmission and, therefore, no trace of a λ_c, although it can be predicted on the basis of theory.

If the metal becomes transparent for $\lambda < \lambda_c$, k must be rather small. Furthermore, from a consideration of Eq. (3), n will be real but less than unity, so that radiation can enter the medium only at angles less than the critical angle, α_c. Hence, for $\lambda < \lambda_c$ metals that have transmission bands or regions will be expected to have a very small k and n less than unity.

4

EXPERIMENTAL METHODS

The metals to be investigated were in the form of thin evaporated films, deposited under optimum conditions as described by Hass, Hunter, and Tousey (8). In the case of unbacked films, a suitable parting agent was placed on the substrate prior to the evaporation of the metal, and another substrate, situated alongside, was exposed during the evaporation and was subsequently coated with silver and used to measure the film thickness by multiple beam interferometry. Details of the process of making unbacked films will be published (9).

The extinction coefficient, k , was measured by transmission through unbacked metal films. By measuring the transmittance of films of different thicknesses, absorption of the surface by an oxide layer, and also reflection losses, can be eliminated, assuming they are the same in both cases. The formula for obtaining k by this method is:

$$k = \frac{\lambda}{4\pi(x_2 - x_1)} \ln_e \frac{T_1}{T_2} \, ,$$

where x is the film thickness and T the transmittance.

If k is very small, and n is less than unity, it is possible to use a technique similar to the critical angle method for measuring the index of non-absorbing solids and liquids in the visible region. Calculations of

reflectance versus angle of incidence for a medium with $n = 0.707$,

$\alpha_c \cong 45^o$ and different values of k, shown in Fig. 1, illustrate that

a definite α_c can be observed only if $k = 0$, however, for small

values of k there is a sudden drop in reflectance in the region of α_c.

The index, n, was obtained from the position of maximum slope of the

reflectance versus angle of incidence curve. The position of the angle of

maximum slope, α_m, of the reflectance curves is very close to α_c,

but moves further away as k increases. Eventually k becomes large

enough so that the R vs α curve is monotonic, as is the case for $k > 0.2$.

Further calculations were made to find the dependence of α_m on k.

The results are shown in Fig. 2, where the angle of incidence of α_m is

shown as a function of k for different values of the index. The curves

for $n \geq 0.7$ are terminated when the respective R vs α curves become

monotonic. By means of these curves a correction for the value of

$n = \sin \alpha_m$ can be determined if k is known for the material. For

example, if the measured value of $\alpha_m = 49.5^o$, and $k = 0.2$, Fig. 2

indicates that $n = 0.6$; neglect of the correction would yield $n = 0.76$,

an error of about 27%. Polarization would cause the measured n to vary

between 0.68 for complete s-polarization and 0.81 for complete p-polariza-

tion, corresponding to errors of 15% and 33%, respectively. This is, of

course an extreme case; corrections for $k \neq 0$ are usually quite small.

The effect of reflections from the metal-substrate interface and the oxide layer are discussed elsewhere (10) and were shown to be, for the most part, negligible.

RESULTS

The results for aluminum are shown in Fig. 3. In the upper part of the figure, the dots through which a solid line has been drawn, represent measured values of $\sin \alpha_m$. The large shaded circles, at 584 Å and 736 Å, are the results of previous measurements (11) using an interference technique. At the same wavelengths, the triangles are data obtained by Madden, Canfield, and Hass (12) from oxide-free surfaces using the general reflectance method. Data obtained by LaVilla and Mendlowitz (13) from inelastic electron scattering experiments are shown as crosses.

Index measurements could only be carried out to 200 Å because, at shorter wavelengths, $\alpha_m > 84°$, which was the largest angle at which measurements could be made. The open circles represent n calculated from the free electron theory using $\lambda_c = 837$ Å and $\tau = 1.1 \times 10^{-15}$ seconds (14), and are in very good agreement with the measured values. From 700 Å to longer wavelengths, the broken curve represents the correction necessary because of the displacement of α_m by the ever-increasing k.

In the lower half of the figure are shown the measured valued of k. The scatter of points is quite large, especially at wavelengths shorter than

7

the $L_{2,3}$ x-ray edge at 170 Å, where the dotted line is to be regarded merely as an indication of the behavior of k. For $\lambda > 170$ Å, the results are somewhat more consistent and the scatter of data decreases with increasing wavelength. Once again the large shaded circles represent the results of previous measurements by transmission while the crosses and triangles are data of LaVilla and Mendlowitz and Madden, Canfield and Hass, respectively. The diamonds represent the data of Tomboulian and Bedo (15), obtained photographically using a synchroton as a light source. Values of k, calculated using the free electron theory are so labelled. There is a definite departure from the free electron model in that the measured k does not decrease with decreasing wavelength as rapidly as the calculated values. This is due to the fact that interband transitions at approximately 8000 Å which are not included in the Drude Theory are still exerting a slight influence.

The data of Tomboulian and Bedo show a sharp dip in the value of k at the $L_{2,3}$ edge. Astoin and Vodar (16), who have measured the transmittance of aluminum films have reported a sharp peak in transmittance at the $L_{2,3}$ edge, corresponding to the dip in k observed by Tomboulian and Bedo. Both sets of investigators used aluminum films backed by thin films of zapon or collodion. In the earlier work of Tomboulian and Pell (17) on unbacked aluminum films, 5000 Å thick, the sharp peak was absent. No sharp peak was observed in the present work, although it would have been detected in

spite of the large scatter of the points near the edge.

In Figure 4 are shown the optical properties of aluminum from 100 Å to 6000 Å . Open circles represent values taken from the experimental curves of the preceeding figure, otherwise the data symbols have the same meaning as in the previous figure with the exception of the additional data of Hass and Waylonis (18) for the near ultraviolet and visible, shown as plus signs.

The solid line, drawn through the index data, represents the index calculated using the free electron theory with the parameters given above, and is in very good agreement with the experimental data at all wavelengths. Good agreement is also obtained in the visible region between the data points for k and the calculated values, which are shown by the solid line. At wavelengths shorter than about 800 Å , however, the curve given by the free electron theory drops more rapidly than the experimental values, shown by the open circles, for the reason given earlier. The dotted line is the

reflectance calculated using the free electron theory which agrees very well with the measured values from 6000 Å to 1025 Å . At shorter wavelengths, the reflectance data points, connected by the dashed line, represent calculations from the measured n and k since interference effects present in thin films prevent direct measurements of reflectance.

The true values of n and k still remain to be found in the interval between 1000 Å and 2000 Å. Because of the agreement between calculated and measured reflectances, however, it is expected that the measurements will not show large deviations from those represented by the solid lines.

Indium has two distinct spectral regions where the value of k becomes very small, from 120 Å to shorter wavelengths, the cut-off wavelength could not be determined; and from 744 Å to approximately 1100 Å . Apparatus was not available for index measurements at the very short wavelengths so that only measurements of the extinction coefficient were made. The results are shown in Table II. Because of experimental difficulties, the numbers are accurate only to within 50% .

The optical constants of indium from 744 Å to 1085 Å are shown in Fig. 5, where measured values are represented by dots. The broken line shows the index curve after correction for the effect of non-zero k .

Although the free electron term in the complex dielectric constant is dominant in this region, other terms are not negligible. For example, the

sharp increase in k , which begins approximately at 760 $\overset{\circ}{A}$, indicates

the commencement of an optical absorption process, thus introducing

another term into the complex dielectric constant. This corresponds to

the sudden termination of transmission observed by Walker, Rustgi, and

Weissler (19) and attributed by them to interband transitions. Hence, no

simple two-parameter model can be made to fit the data.

At wavelengths less than 800 $\overset{\circ}{A}$, the location of α_m was uncertain

and the values shown may be in error by 50% or more. An attempt was

made to obtain more accurate values by matching the calculated transmit-

tance to that which was observed by varying n , however, the calculated

transmittance was insensitive to the value of n chosen and the attempt was

abandoned.

The critical wavelength associated with the free electron term, may

be determined from the quantity, $2nk/(n^2 + k^2)^2$ (20, 21) which should have

a sharp peak very close to the position of λ_c . In Fig. 6, this expression

is shown as a function of wavelength for indium and aluminum. The circles

represent experimental points obtained in the present experiment, while

the crosses, for aluminum, are the data of LaVilla and Mendlowitz. The

solid line for aluminum was calculated using n and k obtained from the

free electron theory, while the line for indium is only to connect the data

points, since no model was available for comparison.

Since, in this experiment, the optical constants of indium were measured at wavelengths shorter than the critical wavelength, the peak of the curve could not be located experimentally. By extrapolating the corrected index curve for indium, however, a peak was found at 1080 Å, shown by the dashed line, which agrees very well with the characteristic energy loss reported by Robins (22) at 1097 Å. Similarly, for aluminum the optical data extend only to 800 Å. However, the data of LaVilla and Mendlowitz agree very closely with the calculated curve which has a peak at approximately 840 Å.

The occurrence of optical transmission suggests that λ_c may be found from the onset in transmission. This is a rather inaccurate way in which to determine λ_c since the thickness of the film and the sensitivity of the measuring equipment essentially determine the longest wavelength at which transmittance occurs. For example, Walker, Rustgi, and Weissler have published transmission curves for aluminum and indium, among other metals, and found the onset of transmission to occur at approximately 855 Å and 1100 Å, respectively. In this experiment, transmission measurements could be made to wavelengths as long as 834 and 1085 Å on aluminum and indium, respectively, while Wilkinson (23) has photographed lines close to 1200 Å through indium films.

Mendlowitz (21) has pointed out that the onset of transmission may not

occur at λ_c but at a somewhat shorter wavelength at which k becomes

small enough to permit transmission. He has also investigated the location

of the maximum in the quantity, $2nk/(n^2 + k^2)^2$ and has shown that, for

non-zero damping, the peak occurs at a wavelength longer than λ_c . The

shift is very small for aluminum, amounting to approximately one part in

5000 , and since the curve for indium is quite similar, it is expected that

the maximum is very close to λ_c .

The results for magnesium are shown in Fig. 7. In the upper part of

the figure, the dots through which the solid line has been drawn represent

the measurements of $\sin \alpha_m$. The open circles are calculations using the

free electron theory with the parameters λ_c = 1198 Å and

τ = 1.1 $\times$ 10^{-15} (14). The calculated values agree fairly well with the

measured values, although not as well as in the case of aluminum. The

greater departure of the points from the smooth curve from 600 to 800 Å

is attributed to uncertainties in the measurements. However, some electron

scattering experiments (24) show a broad peak centered at about 20 ev ,

believed to be due to MgO , which may have influenced the results.

The lower part of the figure shows k , calculated using the free electron

theory. Kroger and Tomboulian (25) have reported values of k , measured

using a photographic technique, from 230 Å to 775 Å . Their values, which

were converted from absorption coefficient μ , to extinction coefficient k ,

are shown as diamonds. The values they reported are approximately one order of magnitude larger than those calculated using the free electron theory. In view of the departure of the measured k values of aluminum from those calculated using the free electron theory this behavior does not seem unreasonable. There is also some evidence of structure in their curve, aside from the $L_{2,3}$ x-ray edge at approximately 250 Å , that could not be expected to appear in calculations using the free electron theory.

Since measured values of k with which to correct the index curve are not available, the calculated values have been used. The corrected curve is shown by the broken line in the upper half of the figure.

The results for silicon are shown in Fig. 8, with dots and open circles, measured and calculated, respectively. The crenulated circles are data of Sasaki and Ishiguro (26). At the shorter wavelengths the measured and calculated data agree rather well; however, from approximately 500 Å to longer wavelengths, the corrected index curve drops more rapidly than the calculated values. The corrected curve has the same slope as the data of Sasaki and Ishiguro although the magnitudes are not quite the same.

In the lower part of the figure are shown the calculated values of k using the free electron theory with the parameters indicated. Since the free electron theory does not take x-ray edges into account, the curve does not show the

14

sudden increase in k that must exist at the $L_{2,3}$ edge and possibly at the L_1 edge also. The data of Sasaki and Ishiguro fit the calculated values approximately as far as magnitudes are concerned but the slope is different.

Reflectance data for some of the metals listed in Table I are collected in Fig. 9. The solid lines are the reflectance at normal incidence calculated on the basis of the free electron theory using the parameters given in the figure caption. The data points indicate that the approximation is close for aluminum and germanium. For aluminum, the triangles represent the data of Madden, Canfield, and Hass, while the crosses are the calculated reflectances from the data of LaVilla and Mendlowitz. The diamonds represent data for germanium obtained by Madden (27).

ACKNOWLEDGMENTS

References

1. Zener, C., Nature $\underline{132}$, 968, 1933.

2. Wood, R. W., Nature $\underline{131}$, 582, 1933; Phys. Rev. $\underline{44}$, 353, 1933.

3. Kronig, R. de L., Nature $\underline{133}$, 211, 1934.

4. Drude, P., Theory of Optics, Dover Publ. Co., New York, 1959.

5. Seitz, F., Modern Theory of Solids, McGraw-Hill Publ. Co., New York, 1940.

6. Pines, D., Rev. Mod. Phys. $\underline{28}$, 184, 1956.

7. Canfield, L. R., Hass, G., and Hunter, W. R., Proceedings of this Colloquium.

8. Hass, G., Hunter, W. R., and Tousey, R., J. Opt. Soc. Am. $\underline{46}$, 1009, 1956.

9. Angel, D. W. (To be published.)

10. Hunter, W. R., J. Opt. Soc. Am. (To be published.)

11. Hass, G., Hunter, W. R., and Tousey, R., J. Opt. Soc. Am. $\underline{47}$, 120 (SA17), 1957: Hunter, W. R., Optica Acta $\underline{9}$, 255, 1962.

12. Madden, R. P., Canfield, L. R., and Hass, G., J. Opt. Soc. Am. $\underline{53}$, 620, 1963.

13. LaVilla, R., and Mendlowitz, H., Phys. Rev. Ltrs $\underline{9}$, 149, 1962.

14. LaVilla, R., Private communication.

15. Tomboulian, D. H., and Bedo, D. E., Rev. Sci. Inst. $\underline{26}$, 747, 1955.

16. Astoin, N., and Vodar, B., J. Phys. et Rad. $\underline{14}$, 424, 1953.

17. Tomboulian, D. H., and Pell, E. M., Phys. Rev. $\underline{83}$, 1196, 1951.

18. Hass, G., and Waylonis, J. E., J. Opt. Soc. Am. $\underline{51}$, 719, 1961.

16

19. Walker, W. C., Rustigi, O. P., and Weissler, G. L., J. Opt. Soc. Am. 49, 1471, 1959.

20. Frohlich, H., and Pelzer, H., Proc. Phys. Soc. 75, 664, 1960.

21. Mendlowitz, H., J. Opt. Soc. Am. 50, 739, 1960.

22. Robins, J. L., Proc. Phys. Soc. 79, 119, 1962.

23. Wilkinson, P. G., Private communication.

24. Marton, L., Leder, L. B., and Mendlowitz, H., Adv. in Electronics and Electron Phys. 7, 183, 1955.

25. Kroger, H., and Tomboulian, D. H., Phys. Rev. 130, 152, 1963.

26. Sasaki, T., and Ishiguro, K., Phys. Rev. 127, 1091, 1962.

27. Madden, R. P., The Physics of Thin Films 1, 123, 1963.

28. Handbook of Chemistry and Physics, Chemical Rubber Publ. Co., Cleveland, Ohio, 1959.

29. Sandstrom, A. E., Hanbuch der Physik 30, 78, 1957 (Berlin: Springer-Verlag, Ed. by S. Flugge).

Table I. Critical angle and closest absorption edge for metals with loosely bound valence and tightly bound core electrons.

At. No.	Element	$\lambda_c(\text{Å})$	$M_{4,5}$	M_1	$L_{2,3}$	K
4	Beryllium	639†				110.7 Å**
5	Boron	650*				66.3 Å**
6	Carbon	560*				43.6 Å**
12	Magnesium	1198†			247.9 Å**	
13	Aluminum	837†			170.0 Å**	
14	Silicon	762†			126.5 Å**	
32	Germanium	743†	470 Å††	70 Å**		

† 14 LaVilla, R., Private communication.

* 6 Pines, D.

** 28 Handbook of Chemistry and Physics

†† 29 Sandström, A. E.

Table II. Extinction coefficient, k, and mass absorption coefficient, μ/ρ, of indium

λ (Å)	k	μ/ρ
44.3	0.003	10^4
67	0.003	10^4

LIST OF CAPTIONS

Figure 1. Calculated reflectance versus angle of incidence for $n = 0.707$, $\alpha_c \cong 45^{\circ}$, and different values of k.

Figure 2. Calculated position of the angle of maximum slope, α_m, as a function of k. The full lines are for unpolarized radiation, the dotted lines for the p-component and the dashed lines for the s-component.

Figure 3. Optical constants of aluminum at wavelengths shorter than the critical wavelength.

Figure 4. Optical constants and normal incidence reflectance of aluminum.

Figure 5. Optical constants of indium from $744\ \text{Å}$ to $1085\ \text{Å}$.

Figure 6. $2nk/(n^2 + k^2)^2$ as a function of wavelength for aluminum and indium.

Figure 7. Optical constants of magnesium at wavelengths shorter than the critical wavelength.

Figure 8. Optical constants of silicon at wavelengths shorter than the critical wavelength.

19

Figure 9. Normal incidence reflectance of various metals in the extreme ultraviolet. Data points Δ (12) and x (13) are for aluminum, and ◊ (27) is for germanium. The solid lines were calculated using a Drude type model with the following parameters (14):

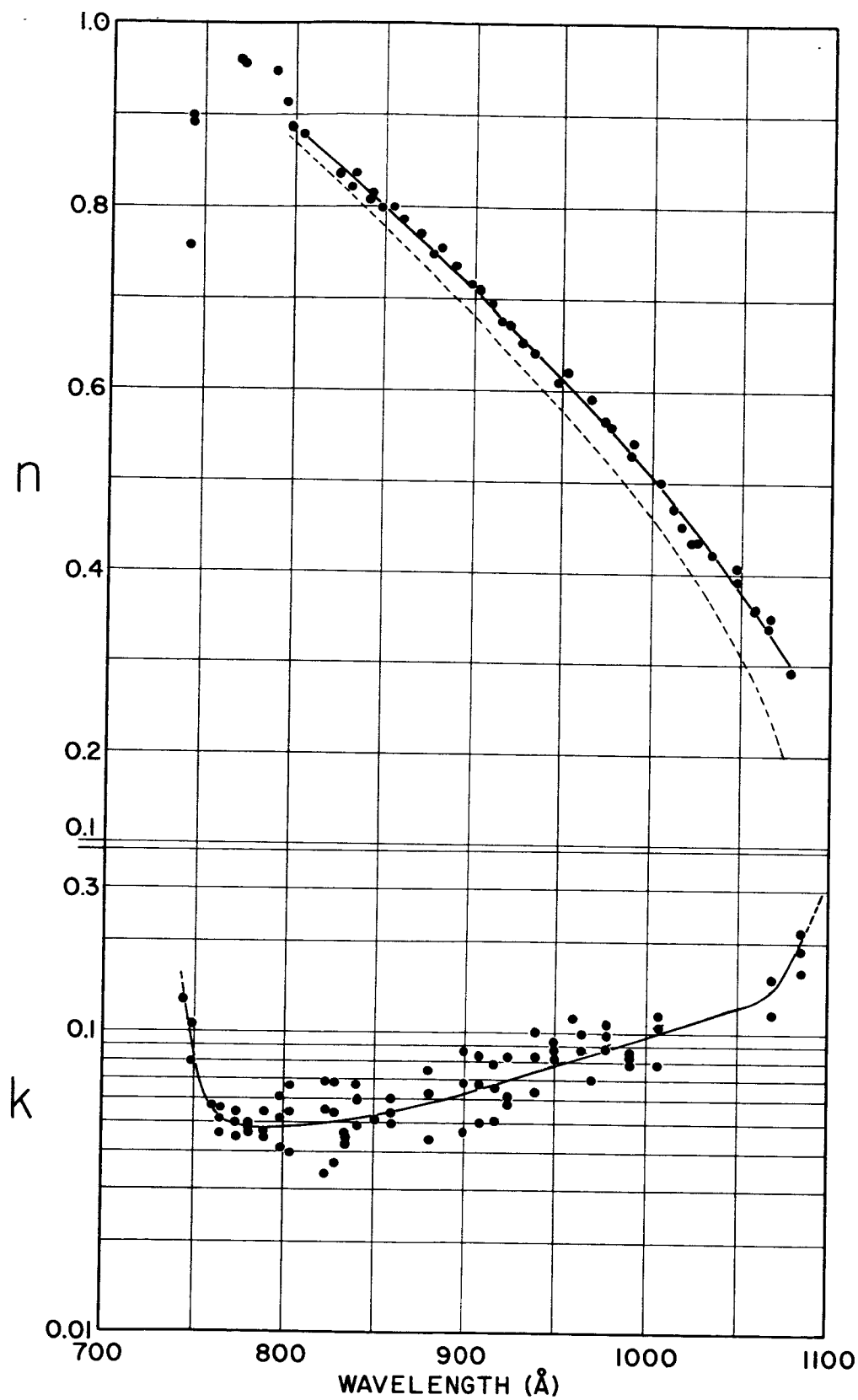|	Be	Al	Mg	Ge	Si
λ_c(Å)	639	837	1198	743	762
τ $(10^{-15}$ sec)	1.3	1.1	1.1	0.16	0.14
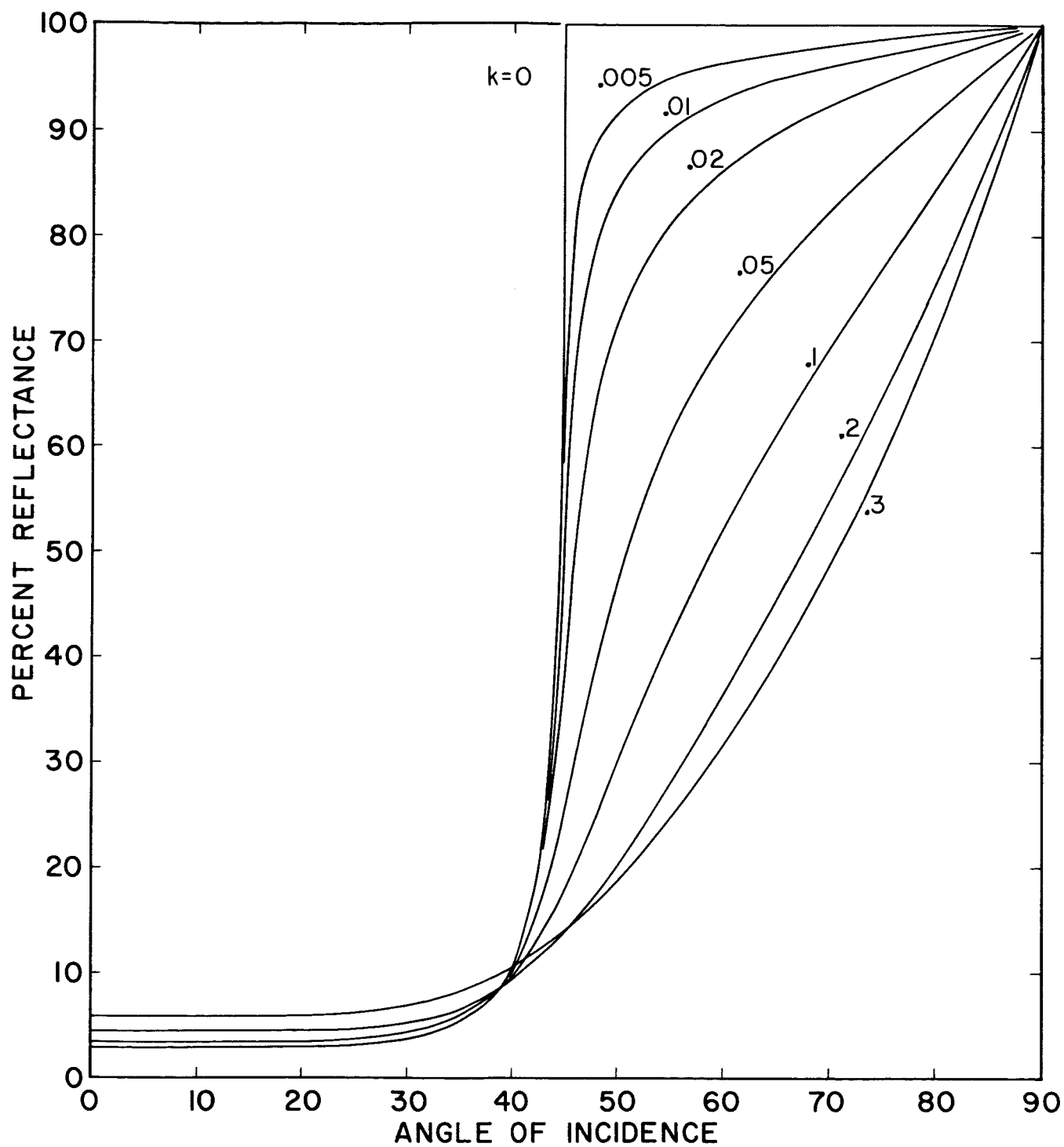
Figure 1
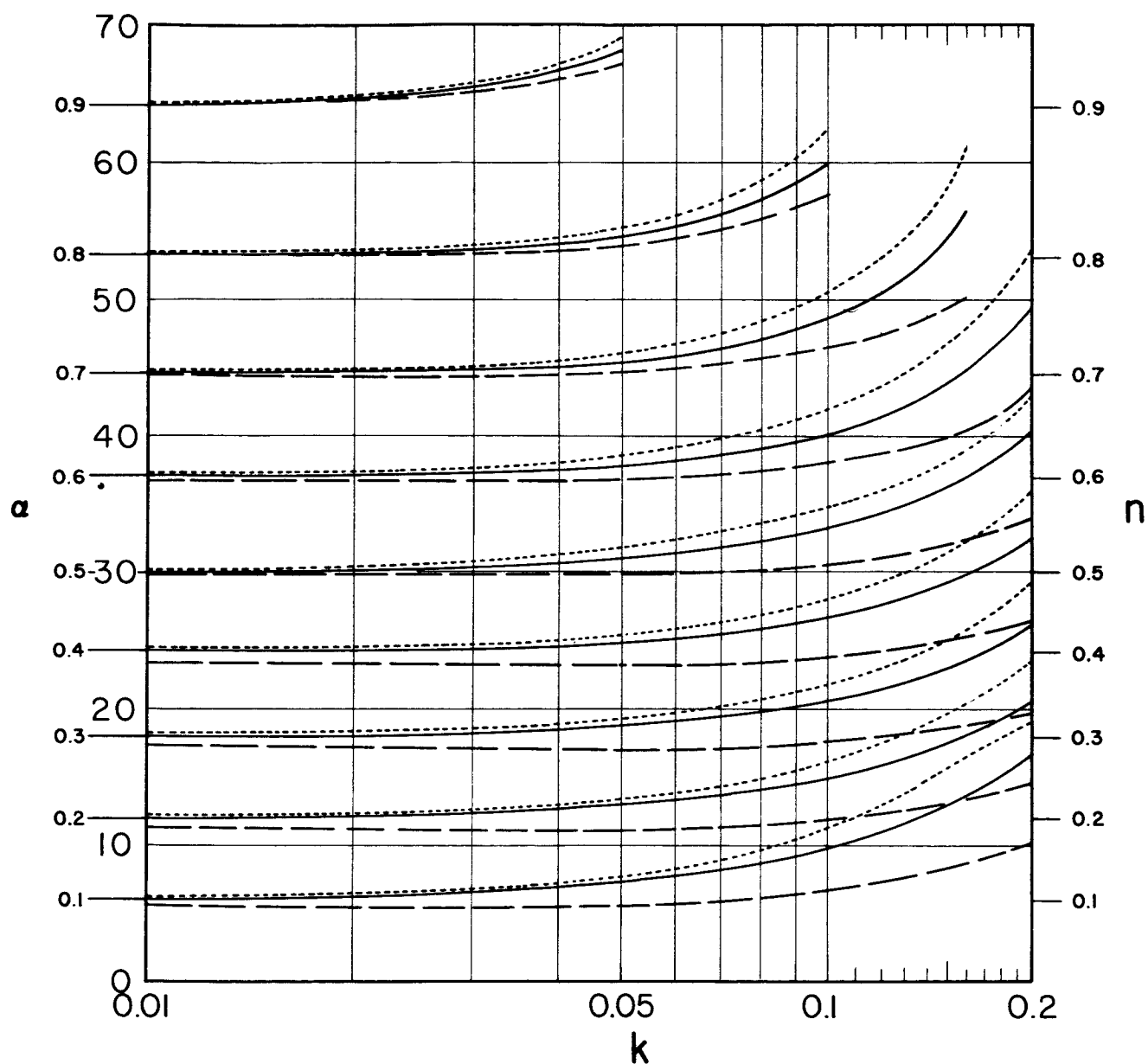
CALCULATED POSITION OF ANGLE OF MAXIMUM SLOPE AS A FUNCTION OF k. ———UNPOLARIZED RADIATION,——— s COMPONENT, ·········p COMPONENT.

Figure 2
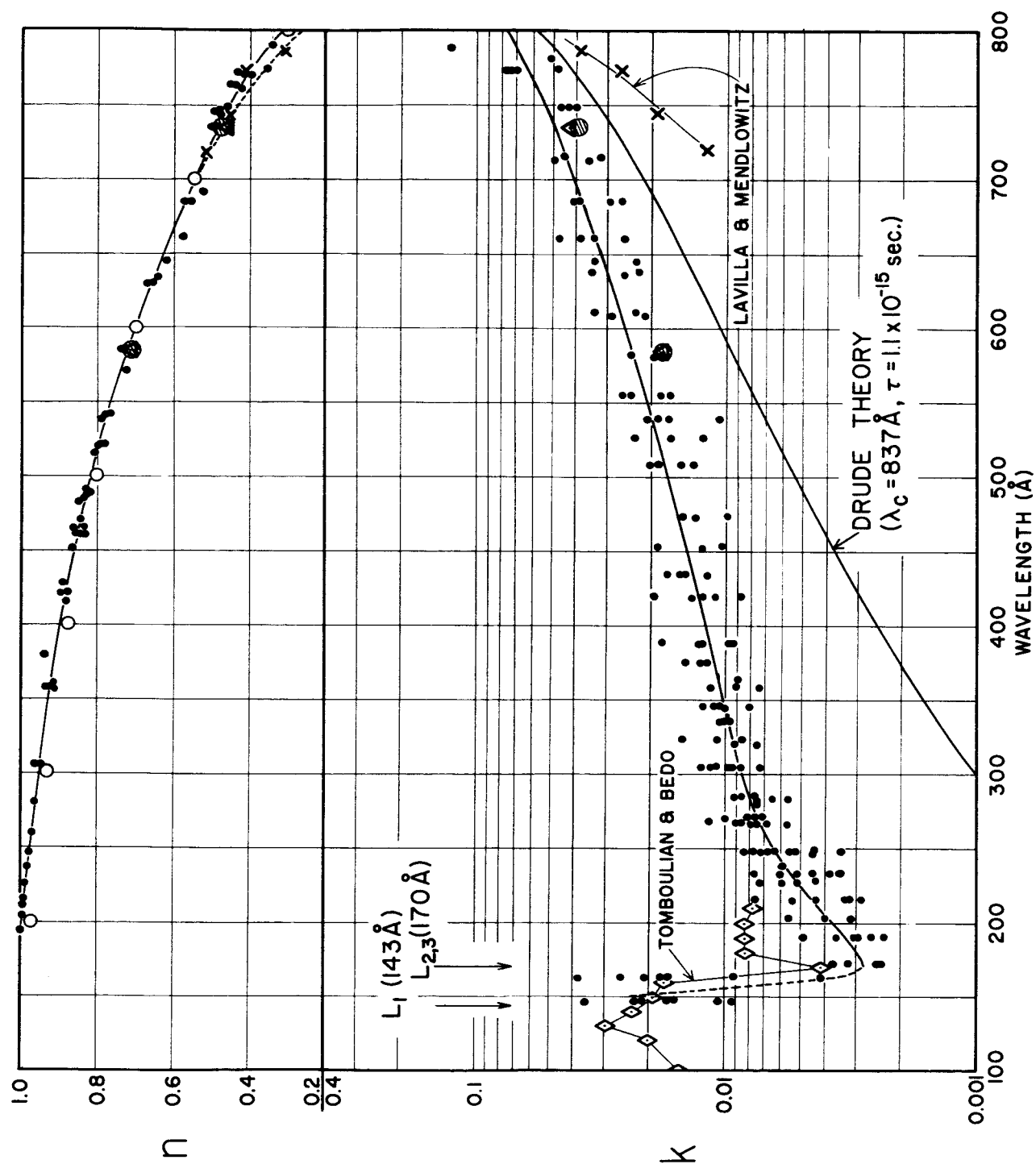
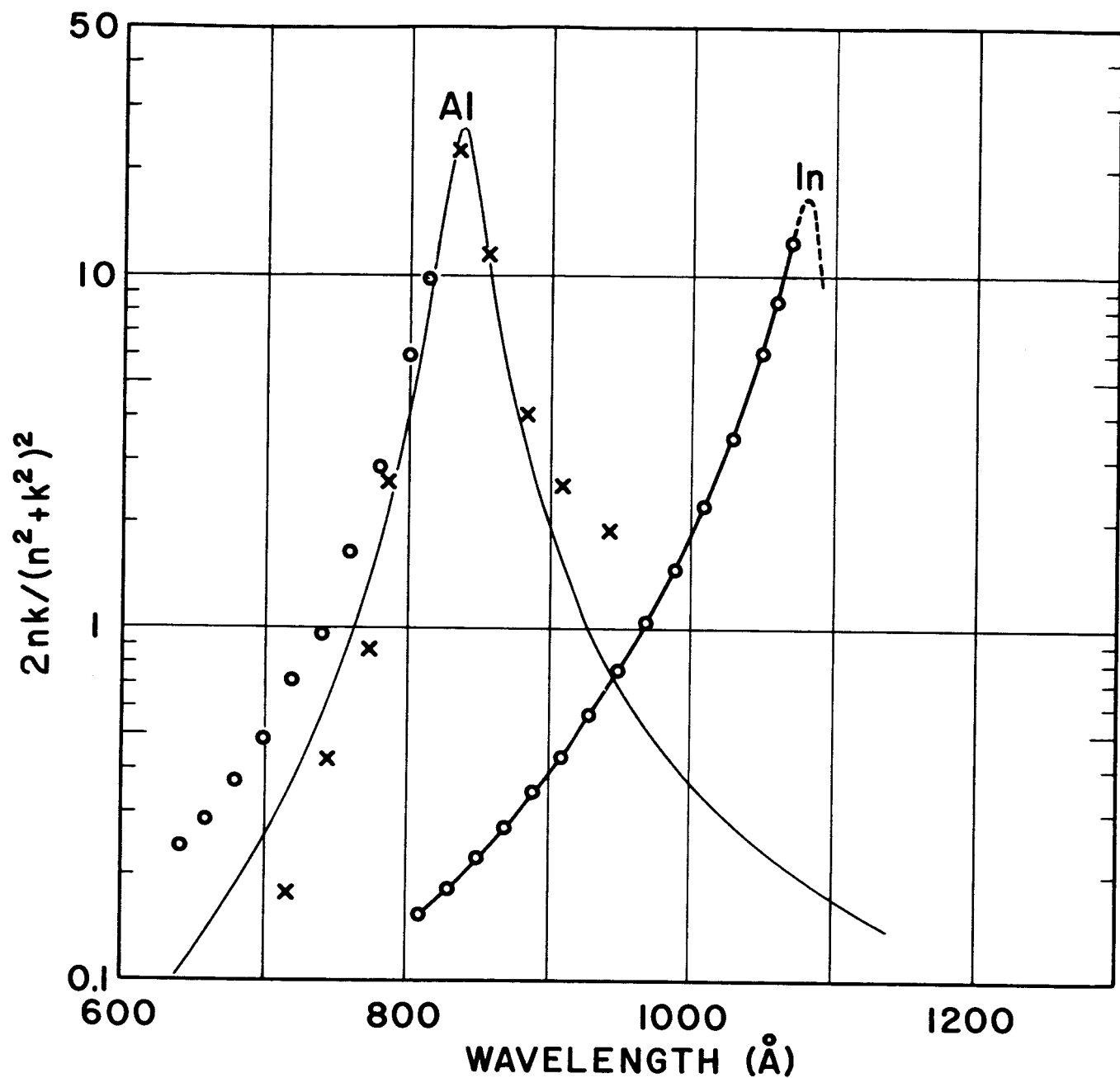OPTICAL CONSTANTS OF ALUMINUM AT WAVELENGTHS SHORTER THAN THE CRITICAL WAVELENGTH.

Figure 3
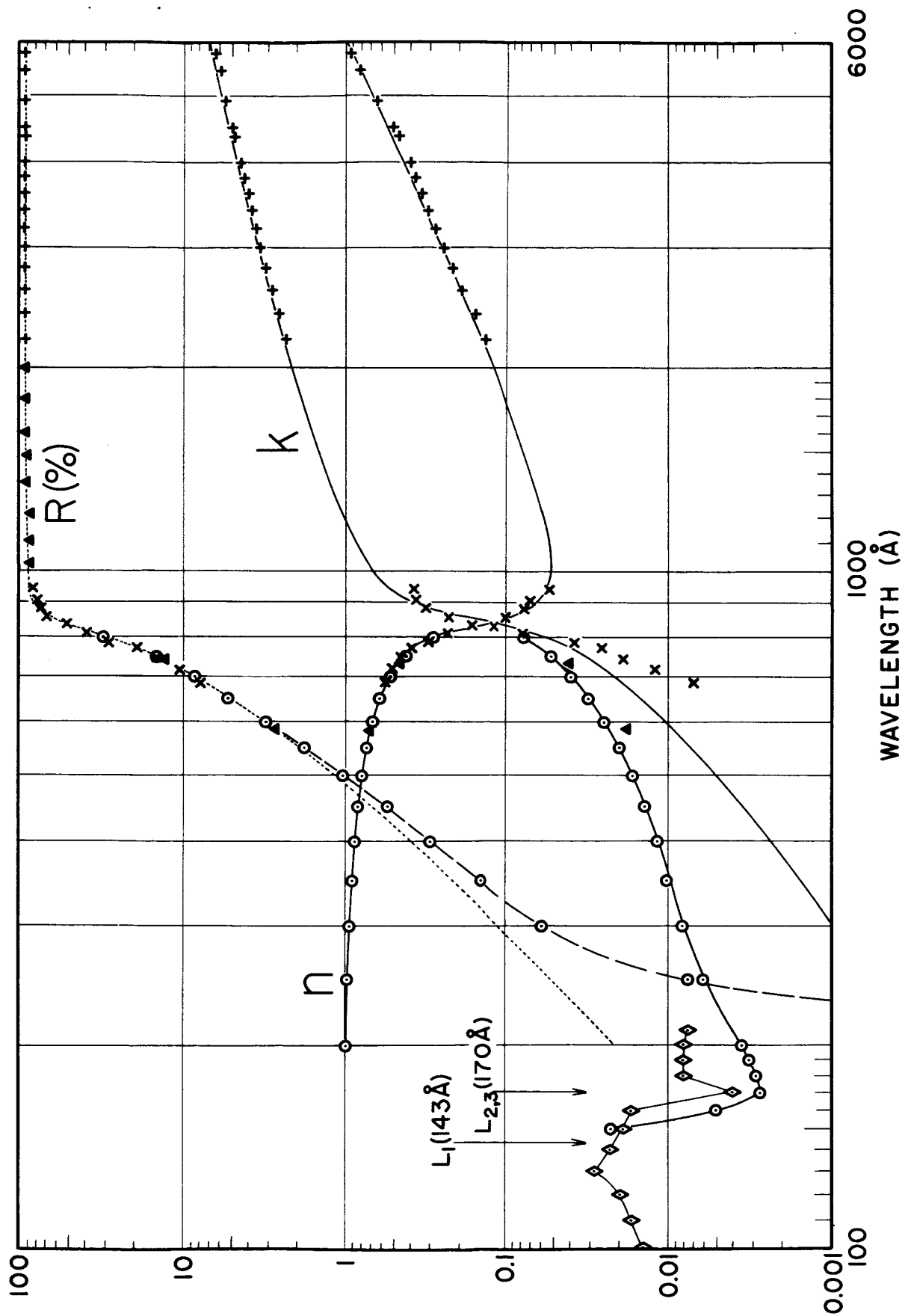
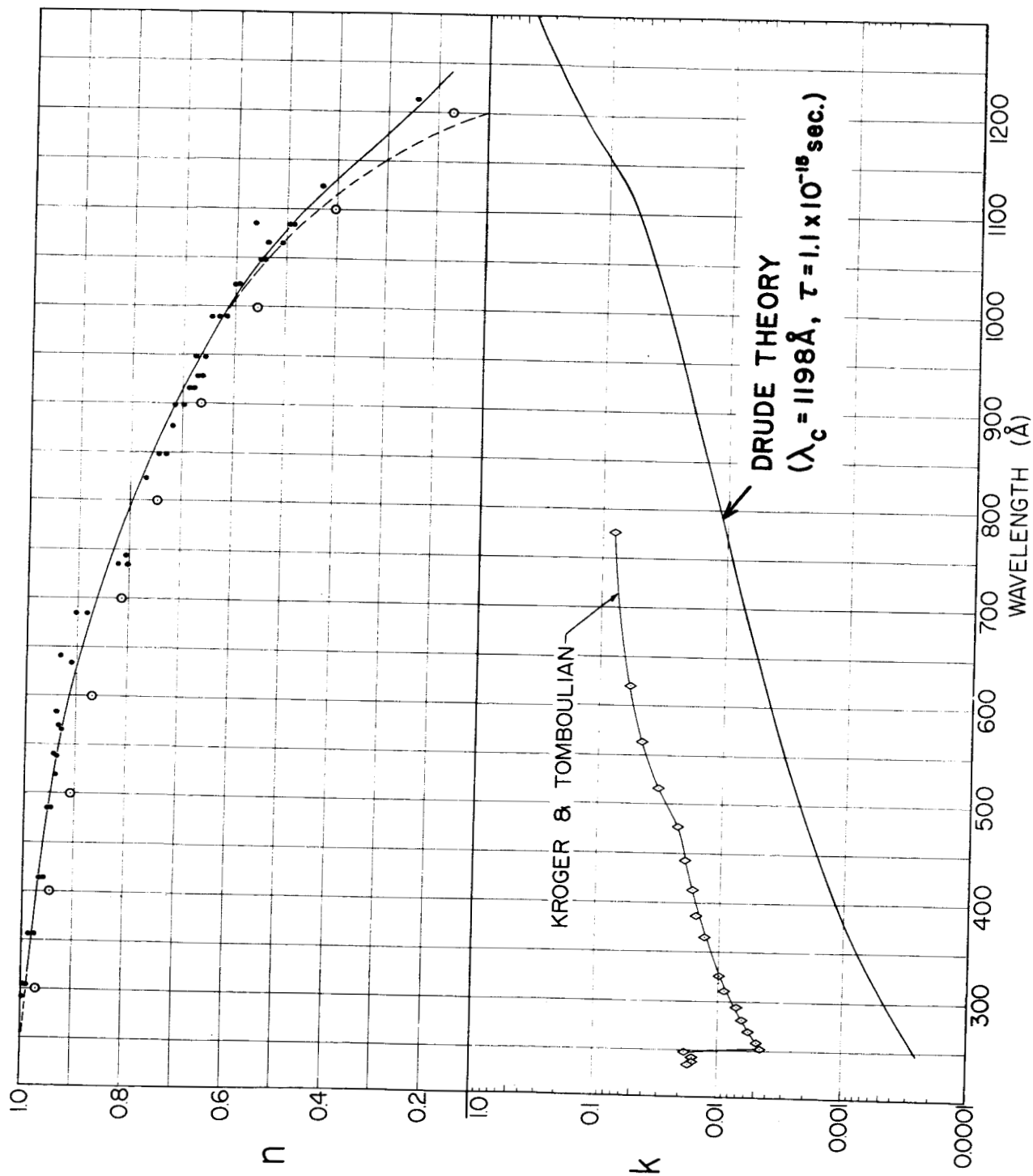OPTICAL CONSTANTS & NORMAL INCIDENCE REFLECTANCE OF ALUMINUM

Figure 4

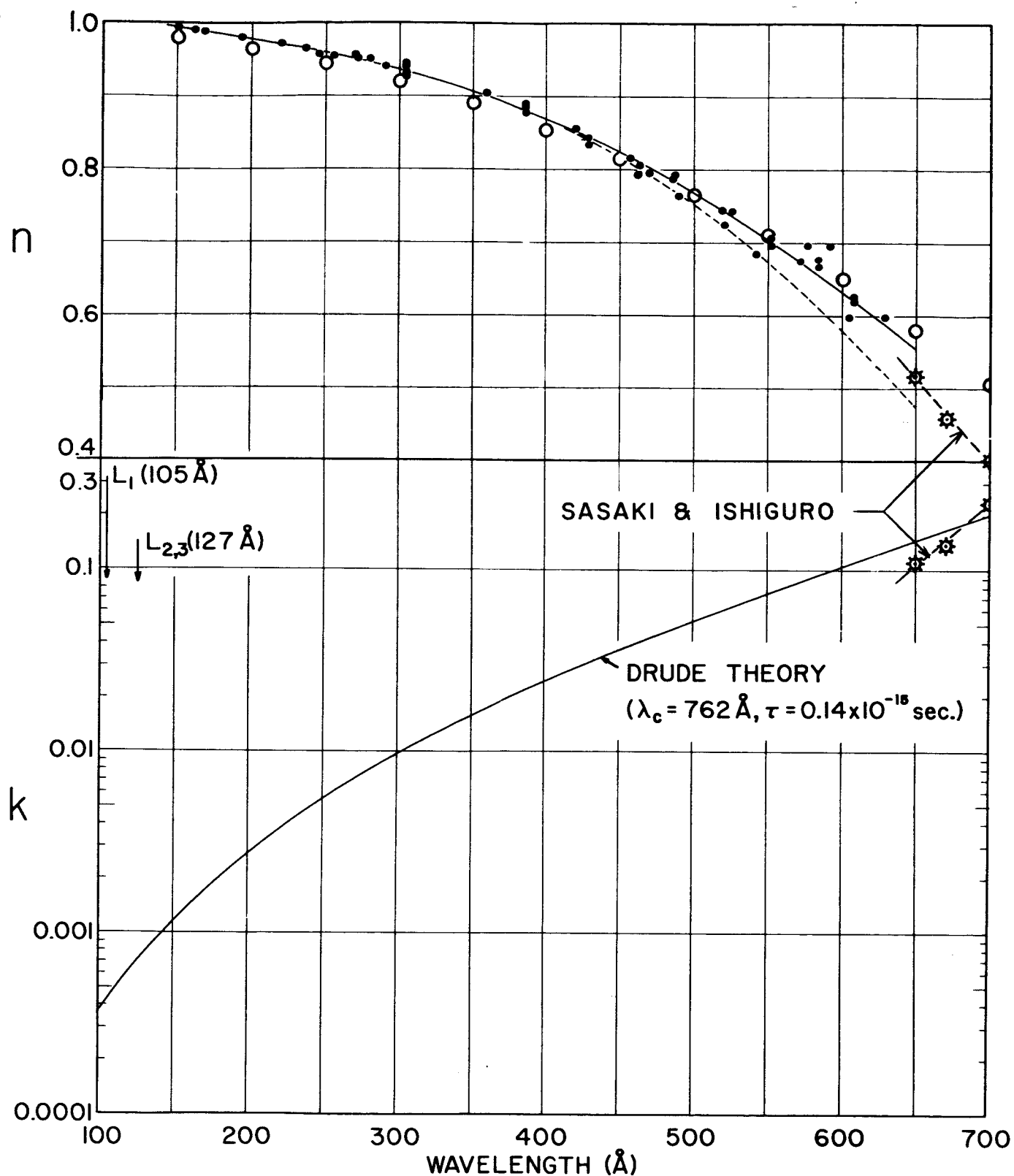OPTICAL CONSTANTS OF INDIUM FROM 744 Å TO 1085 Å.

Figure 5

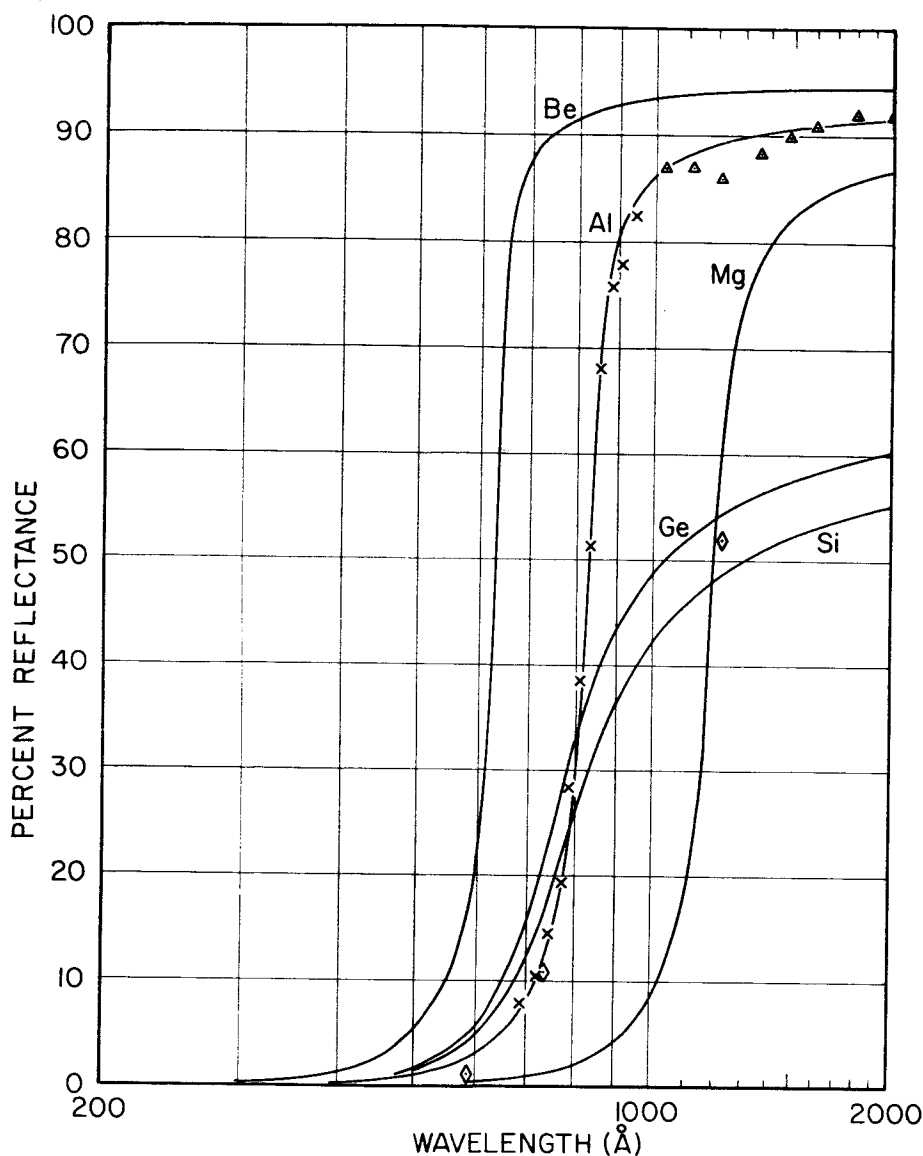2nk/(n²+k²)² AS A FUNCTION OF WAVELENGTH FOR ALUMINUM & INDIUM.

Figure 6

OPTICAL CONSTANTS OF MAGNESIUM AT WAVELENGTHS SHORTER
THAN THE CRITICAL WAVELENGTH

Figure 7

OPTICAL CONSTANTS OF SILICON AT WAVELENGTHS
SHORTER THAN THE CRITICAL WAVELENGTH.

Figure 8

NORMAL INCIDENCE REFLECTANCE OF VARIOUS METALS AND SEMICONDUCTORS IN THE EXTREME ULTRAVIOLET. DATA POINTS × & △ ARE FOR Al AND ◊ IS FOR Ge. THE SOLID LINES WERE CALCULATED USING A DRUDE-TYPE MODEL WITH THE FOLLOWING PARAMETERS;

	Be	Al	Mg	Ge	Si
λ_c(Å)	639	837	1198	743	762
τ(10^{-15} sec.)	1.3	1.1	1.1	0.16	0.14

Figure 9